BAMS Article

Global Ocean Monitoring and Prediction at NOAA Climate Prediction Center

15 Years of Operations

Zeng-Zhen Hu, Yan Xue, Boyin Huang, Arun Kumar, Caihong Wen, Pingping Xie, Jieshun Zhu, Philip J. Pegion, Li Ren, and Wanqiu Wang

ABSTRACT: Climate variability on subseasonal to interannual time scales has significant impacts on our economy, society, and Earth's environment. Predictability for these time scales is largely due to the influence of the slowly varying climate anomalies in the oceans. The importance of the global oceans in governing climate variability demonstrates the need to monitor and forecast the global oceans in addition to El Niño–Southern Oscillation in the tropical Pacific. To meet this need, the Climate Prediction Center (CPC) of the National Centers for Environmental Prediction (NCEP) initiated real-time global ocean monitoring and a monthly briefing in 2007. The monitoring covers observations as well as forecasts for each ocean basin. In this paper, we introduce the monitoring and forecast products. CPC's efforts bridge the gap between the ocean observing system and the delivery of the analyzed products to the community. We also discuss the challenges involved in ocean monitoring and forecasting, as well as the future directions for these efforts.

KEYWORDS: Ocean; Atmosphere-ocean interaction; ENSO; Climate prediction; Oceanic variability; Climate services

https://doi.org/10.1175/BAMS-D-22-0056.1

Corresponding author: Zeng-Zhen Hu, zeng-zhen.hu@noaa.gov

In final form 15 August 2022

AFFILIATIONS: Hu, Kumar, Wen, Xie, Zhu, Ren, and Wang—Climate Prediction Center, NOAA/NWS/NCEP, College Park, Maryland; **Xue**—Office of Science and Technology Integration, NOAA/NWS, Silver Spring, Maryland; **Huang**—National Centers for Environmental Information, Asheville, North Carolina; **Pegion**—Cooperative Institute for Research in Environmental Sciences, University of Colorado Boulder, and NOAA/ESRL/Physics Sciences Division, Boulder, Colorado

Climate variations on subseasonal to interannual time scales have significant impacts on different facets of society. Knowing the variations in advance is important for decision-makers and emergency managers. It has been well established that the predictable component of climate variability primarily comes from the influence of slowly evolving climate anomalies in the oceans (National Research Council 2010). For instance, sea surface temperature anomalies (SSTAs) in the central and eastern tropical Pacific associated with El Niño–Southern Oscillation (ENSO; McPhaden et al. 2021) have a considerable influence on precipitation in many tropical and extratropical regions (Ropelewski and Halpert 1987; Hu et al. 2020a; Li et al. 2022). During El Niño (La Niña) years, a wet (dry) winter is favored in the southern parts of North America (Ropelewski and Halpert 1987) and southeastern China (Wu et al. 2003), and an inactive (active) summer monsoon is expected in the Indian Peninsula (Rasmusson and Carpenter 1983). Moreover, ENSO is also an important factor in modulating the variability of typhoons in the northwestern Pacific (Han et al. 2016) and hurricanes in the North Atlantic (Gray 1984).

SSTAs in the other ocean basins also play an active role in influencing regional climate variability. SSTAs in the tropical North Atlantic Ocean are a crucial predictor of hurricane activity in the Atlantic (e.g., Wang et al. 2014). SSTAs in the Indian Ocean can affect the Indian summer monsoon (e.g., Cherchi et al. 2007) and climate variations in South China (e.g., Wu et al. 2003). Furthermore, the oceanic temperature anomaly along the coastal regions can impact biological productivity, such as the fisheries in the California coastal regions (Ware and McFarlane 1989).

The importance of the global oceans in climate variability and predictability led to the development of a global ocean observing system that includes both in situ and satellite observation platforms that monitor physical, chemical, or biological variables contributing to the characterization of Earth's climate (Bojinski et al. 2014; Moltmann et al. 2019). In recent decades, considerable advances have been made in the in situ ocean observing systems. For example, ocean observations from Argo floats now provide extensive observations across the global oceans with core Argo floats sampling from the surface to 2,000 m and deep Argo floats sampling to 4,000 or 6,000 m (e.g., Roemmich et al. 2019). A comprehensive set of ocean observations is routinely provided to operational centers that ingest them in the ocean and atmospheric data assimilation systems to support climate monitoring and prediction activities. As a product of the data assimilation systems, a three-dimensional rendition of the ocean state on a regular grid has greatly advanced our understanding of ocean variability and air–sea interactions (Fujii et al. 2019).

The full utility of the ocean observing system can only be realized from an end-to-end ocean climate information system that includes (i) collecting ocean observations, (ii) methods to convert them into data products that are readily usable by the user community, and (iii) a routine delivery of synthesis information about the current state of the ocean and its near-time evolution.

To meet the last requirement, with the support of the Climate Program Office (CPO) of the National Oceanic and Atmospheric Administration (NOAA), the Climate Prediction Center (CPC) of the National Centers for Environmental Prediction (NCEP) in 2007 initiated activity for disseminating the real-time global ocean monitoring and forecast information. This activity is also complemented by a monthly briefing that is open to all interested users. With the ongoing support of the Global Ocean and Monitoring of Observations (GOMO) program, this effort continues to date.

CPC's ocean monitoring and forecast effort provides direct or indirect support to various operational products including ENSO, hurricane, monthly and seasonal U.S. precipitation and temperature, and drought outlooks within NOAA and the academic community. Through monitoring the reanalyses, the Climate Forecast System Reanalysis (CFSR) and the Global Ocean Data Assimilation System (GODAS) at NCEP, we continuously validate the products which provide initial conditions to the NCEP Climate Forecast System version 2 (CFSv2). Outside of NCEP, these products are widely used in supporting climate services and research. The ocean briefing plots have also been used as teaching materials for college and graduate students.

In this report, to provide additional visibility for our effort, and to seek feedback from a broader user community, we summarize the monitoring and forecast products. The paper is organized as follows: the second section highlights monitoring products, the third section summarizes ocean forecast products and monitoring of the ocean observing system, and the fourth section discusses the challenges and outlines the future direction. The observational, reanalysis, and forecast datasets used for supporting this activity are described in the appendix.

Monitoring of global and individual ocean basins

Global ocean. Monitoring essential climate variables over the global oceans provides a broad overview of the current state of the ocean. The general focus of the monitoring documents anomalies and their temporal tendencies (to depict their evolution in the few months leading up to the present, e.g., Fig. 1b) for different variables. Here, monthly, weekly, and pentad anomalies are referenced to the corresponding climatologies in 1991–2020. The anomalies for which spatial distribution is monitored include

- SST (Fig. 1a),
- sea surface height (SSH),
- ocean heat content (OHC),
- OHC in the upper 300 m (OHC300),
- subsurface ocean temperature along the equator,
- ocean mixed layer depth, and
- tropical cyclone heat potential (TCHP).

To complement the spatial patterns of anomalies, we also monitor the temporal evolution of spatially averaged SSTAs in various ocean basins, including the global, tropical and North Pacific, tropical and North Atlantic, and Southern Oceans (i) starting in 1950 and 1982, (ii) during last four years, and (iii) during last 13 months. Similar monitoring activities are also made for SSH anomalies for periods (i) since the advent of satellite altimetry (i.e., 1993; Pujol et al. 2016) and (ii) during the last 4 years.

Tropical and North Pacific. The primary focus of ENSO monitoring and its evolution is various area-averaged Niño indices: the Niño1+2, Niño-3, Niño-3.4, and Niño-4 (Barnston et al. 1997). Sustained warm/cold Niño-3.4 values are indicative of an El Niño/La Niña event

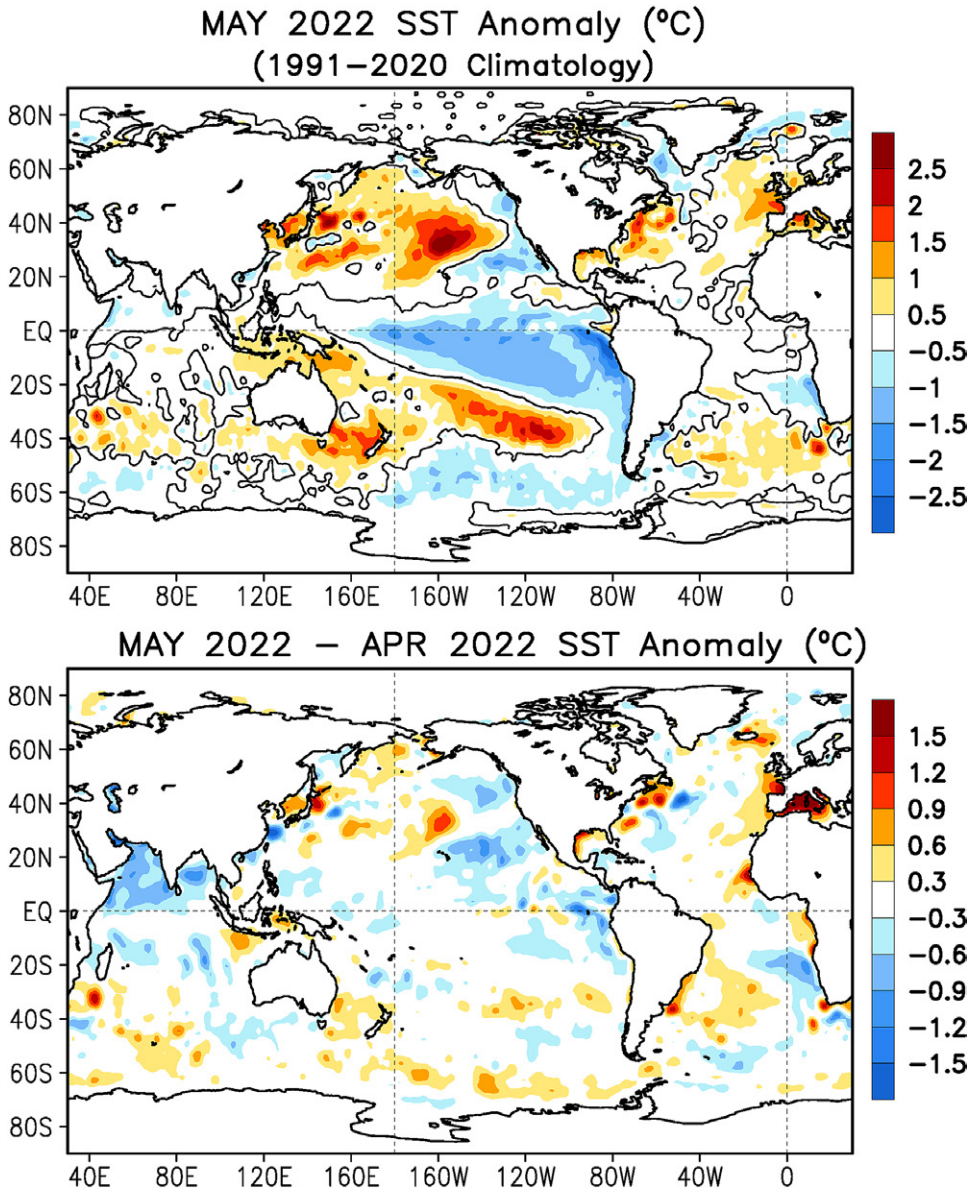

Fig. 1. Optimal Interpolation version 2.1 (OIv2.1) monthly SSTAs (°C) of (top) the global oceans in February 2022 and (bottom) the tendencies, which are the differences in SSTAs between February and January 2022.

in the eastern equatorial Pacific. In addition, routine monitoring of other ENSO indices is also maintained including the ENSO-Modoki (Ashok et al. 2007), cold tongue (Ren and Jin 2011), warm pool (Ren and Jin 2011), and the relative Niño-3.4 (van Oldenborgh et al. 2021). These indices are included to discern different flavors of ENSO (Fig. 2) (McPhaden et al. 2021). In the peak phase of an El Niño, the so-called eastern (central) Pacific event is associated with a large positive anomaly in the cold tongue (warm pool or ENSO-Modoki) index.

Previous analysis has indicated that the ENSO SST variability has precursors that are related to the integrated measure of basinwide averages of subsurface thermal conditions across the equatorial Pacific. For example, the ENSO SST anomalies are related to the temporal evolution in the subsurface warm water volume (WWV) in the equatorial Pacific quantified by the WWV index (Meinen and McPhaden 2000), which is a proxy of the recharge/discharge oscillator paradigm for the phase transition of the ENSO cycle (Jin 1997). Statistically, a positive (negative) WWV index leads El Niño (La Niña) by a few seasons (Meinen and McPhaden 2000). As part of the ocean monitoring effort, the temporal evolution of the equatorial ENSO precursors is included. In addition, the projection of the ocean temperature anomalies (OTAs) onto two

leading empirical orthogonal function (EOF) modes are updated routinely (Fig. 3; Kumar and Hu 2014). For the projection onto the EOF2, the OTAs in various longitudes and depths are weighted on their leading EOF patterns, implying spatially heterogeneous contributions of ocean temperature to the WWV variation, which is not considered in the conventional WWV index definition.

High-frequency variations associated with oceanic Kelvin wave and westerly wind bursts are an important factor modulating ENSO evolutions. To detect the intraseasonal to seasonal variations in the ocean, we monitor both oceanic Kelvin wave activity along the equatorial Pacific based on the methodology of Seo and Xue (2005) with GODAS pentad ocean temperature (Fig. 4), and pentad OTAs from the Tropical Atmosphere Ocean (TAO) analysis from the Tropical Ocean Global Atmosphere program (McPhaden et al. 1998) and GODAS. In the oceanic Kelvin wave index (Fig. 4), the eastward propagation of the positive (negative) anomalies corresponds to the downwelling warm (upwelling cold) Kelvin wave, which favors the development of El Niño (La Niña). Here, the oceanic Kelvin wave index is defined as standardized projections of pentad OTAs onto the 14 patterns of extended EOF1 (EEOF1) of equatorial OTAs of upper 300 m following Seo and Xue (2005). Furthermore, to qualify the contributions of different dynamical and thermodynamic processes in SSTAs, different terms of oceanic mixed layer heat budget are also diagnosed and updated for each pentad based on the GODAS output (Huang et al. 2010, 2012; Hu et al. 2016).

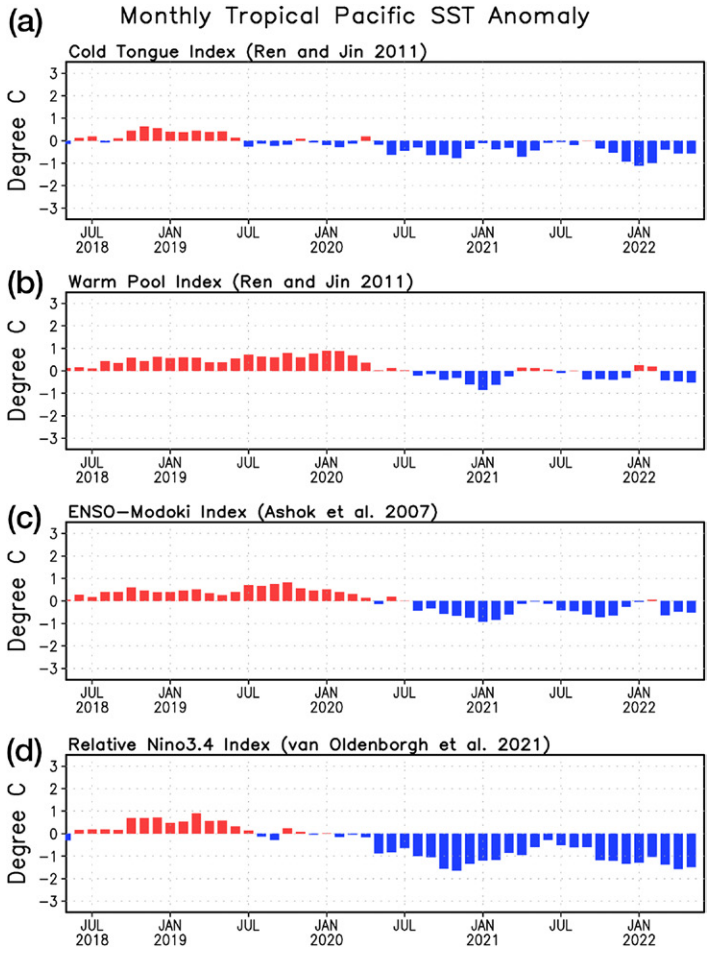

Fig. 2. OIv2.1 monthly SSTAs (°C) of (a) cold tongue, (b) warm pool, (c) ENSO-Modoki, and (d) relative Niño-3.4 indices in the last four years.

The monitoring of the tropical Pacific also includes time–longitude evolution of pentad anomalies of surface zonal current, SST, OHC, zonal wind at 850 hPa (U850), and velocity potential at 200 hPa along the equator. These variables are of importance in monitoring the air–sea coupled evolution along the equator. In addition to the time–longitude section, the spatial patterns of monthly anomalies of SST, SST tendency, year-to-year change in SST, outgoing longwave radiation (OLR), winds at 925 and 200 hPa, and ocean surface heat flux during the latest 3 months are also monitored.

Other monitored variables in the North Pacific include the spatial pattern of monthly SSTA, weekly SSTA tendency, OLR, sea level pressure (SLP), and ocean surface heat flux anomalies (Fig. 5), as well as the monthly anomalies of SST, OLR, and wind at 925 hPa during the latest 3 months. From these variables, we can discern the contributions of dynamic and thermodynamic processes to the SSTA evolution. Furthermore, based on GODAS, the pentad means of upwelling and downwelling along the northeastern Pacific coast between 20° and 60°N

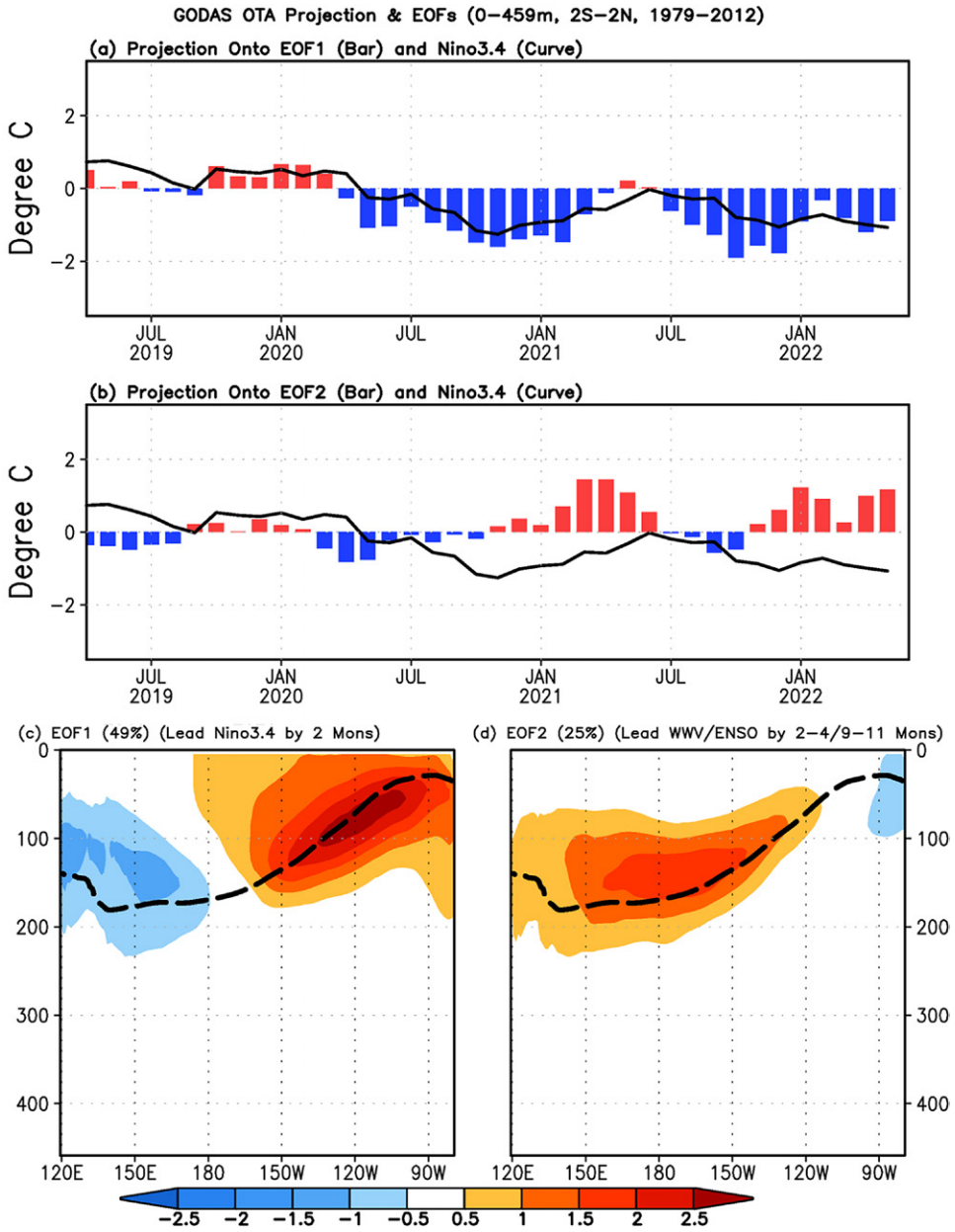

Fig. 3. (a),(b) The bars are the projection coefficients of the GODAS monthly ocean temperature anomalies (OTAs) onto the (c) EOF1 and (d) EOF2, respectively. The lines in (a) and (b) are the OIv2.1 monthly Niño-3.4 index (°C). The lines in (c) and (d) are the climatological depth of the 20°C isotherm (D20), which represents the depth of the oceanic mixed layer.

(important modulators for fishery production; Ware and McFarlane 1989) during the last 13 months and 4 years are updated routinely.

In the North Pacific, the Pacific decadal oscillation (PDO) is crucial for the regional climate and marine ecosystems (Mantua et al. 1997), and monitored through (i) an SST-based PDO index (SPDOI), and (ii) an OHC300-based PDO index (HPDOI) updated monthly (Kumar and Wen 2016). SPDOI is the standardized projection of the monthly SSTAs onto the first EOF pattern of North Pacific SSTA, while HPDOI is defined as the projections of monthly OHC300 anomalies from GODAS onto the first EOF of the North Pacific (20°–60°N) OHC300 variability. HPDOI provides a natural way to highlight the lower-frequency variability in the SPDOI. It is also noted that on average, HPDOI lags SPDOI by a few months following the downward propagation of PDO-associated temperature from the ocean surface to the subsurface.

The Indian Ocean. There are two main modes of SSTA variability in the tropical Indian Ocean: the Indian Ocean dipole mode (IOD; Saji et al. 1999) and the Indian Ocean basin mode (IOBM; Chambers et al. 1999). The IOD index, and its corresponding southeastern (SETIO) and western (WTIO) nodes, as well as the IOBM index, are monitored for their evolutions since 1950 and 1982, and during the latest four years (Fig. 6), respectively. When the IOD index is positive (negative), the warming (cooling) in WTIO is larger than that in SETIO, and surface easterly (westerly) wind anomalies prevail. The monitoring products also include the spatial patterns of monthly anomalies of SST, SST tendency, year-to-year change in SST, OLR, wind at 925 and 200 hPa, temporal and longitude evolutions of pentad anomalies of SST, OHC, U850 anomalies along the equatorial Indian Ocean and 10°S, as well as the monthly anomalies of SST, OLR, and wind at 925 hPa during the latest 3 months. These oceanic and atmospheric variables together help us to understand the coupled air–sea interactions in the Indian Ocean, such as IOBM and IOD-like variability.

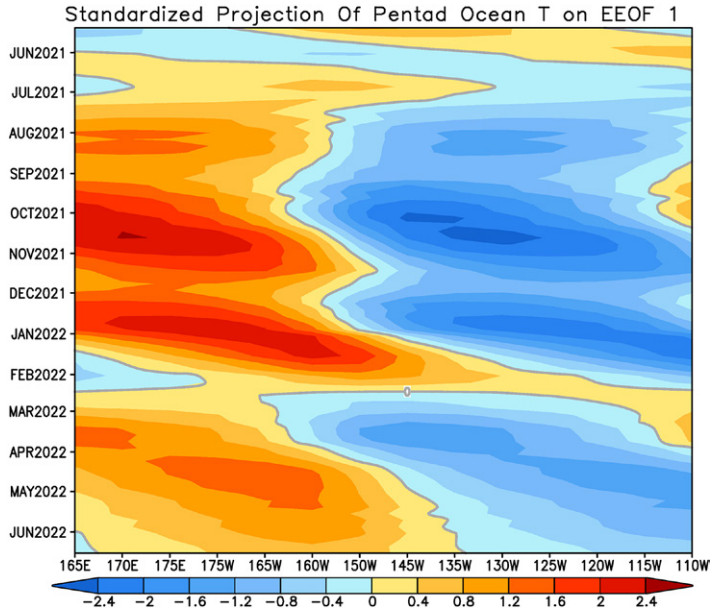

Fig. 4. Oceanic Kelvin wave index along the equatorial Pacific Ocean calculated based on GODAS pentad OTAs.

The Atlantic and Arctic Oceans. For the tropical and North Atlantic Ocean, temporal evolutions of multiple indices are monitored, including the ATL3 (Zebiak 1993), tropical North Atlantic (TNA), tropical South Atlantic (TSA), and meridional gradient (TNA–TSA; Enfield et al. 1999) indices (Fig. 7). The ATL3 is a key index to measure the equatorial Atlantic Niño evolution and the TNA index is an indicator of Atlantic hurricane activity. The monthly North Atlantic Oscillation (NAO) index (NAOI), calculated based on Barnston and Livezey (1987), is included as a monitoring component. Together with the NAO, the evolution of the zonal SSTA of the tropical and North Atlantic Ocean is monitored as well.

Similar to the other ocean basins, the spatial patterns of monthly anomalies of SST, SST tendency, year-to-year change in SST, OLR, wind at 925 and 200 hPa, ocean surface heat flux, as well as the monthly anomalies of SST, OLR, and wind at 925 hPa during the latest 3 months in both the tropical and North Atlantic Ocean are also provided. For the tropical Atlantic Ocean, wind shear between 200 and 850 hPa, relative humidity at 700 hPa, and TCHP are monitored. The monitoring of these quantities routinely updates the status of the environmental conditions that modulate hurricane development in the tropical North Atlantic Ocean and, therefore, is important during the hurricane peak season that extends from August to October.

For the Arctic Ocean, based on the analyses of the National Snow and Ice Data Center (http://nsidc.org/arcticseaicenews/), we discuss the monthly sea ice extent, historical ranking, as well as the possible atmospheric drivers of the sea ice anomalies. That provides a basis for CPC Arctic sea ice prediction verification (www.cpc.ncep.noaa.gov/products/people/wwang/seaice_seasonal/index.html).

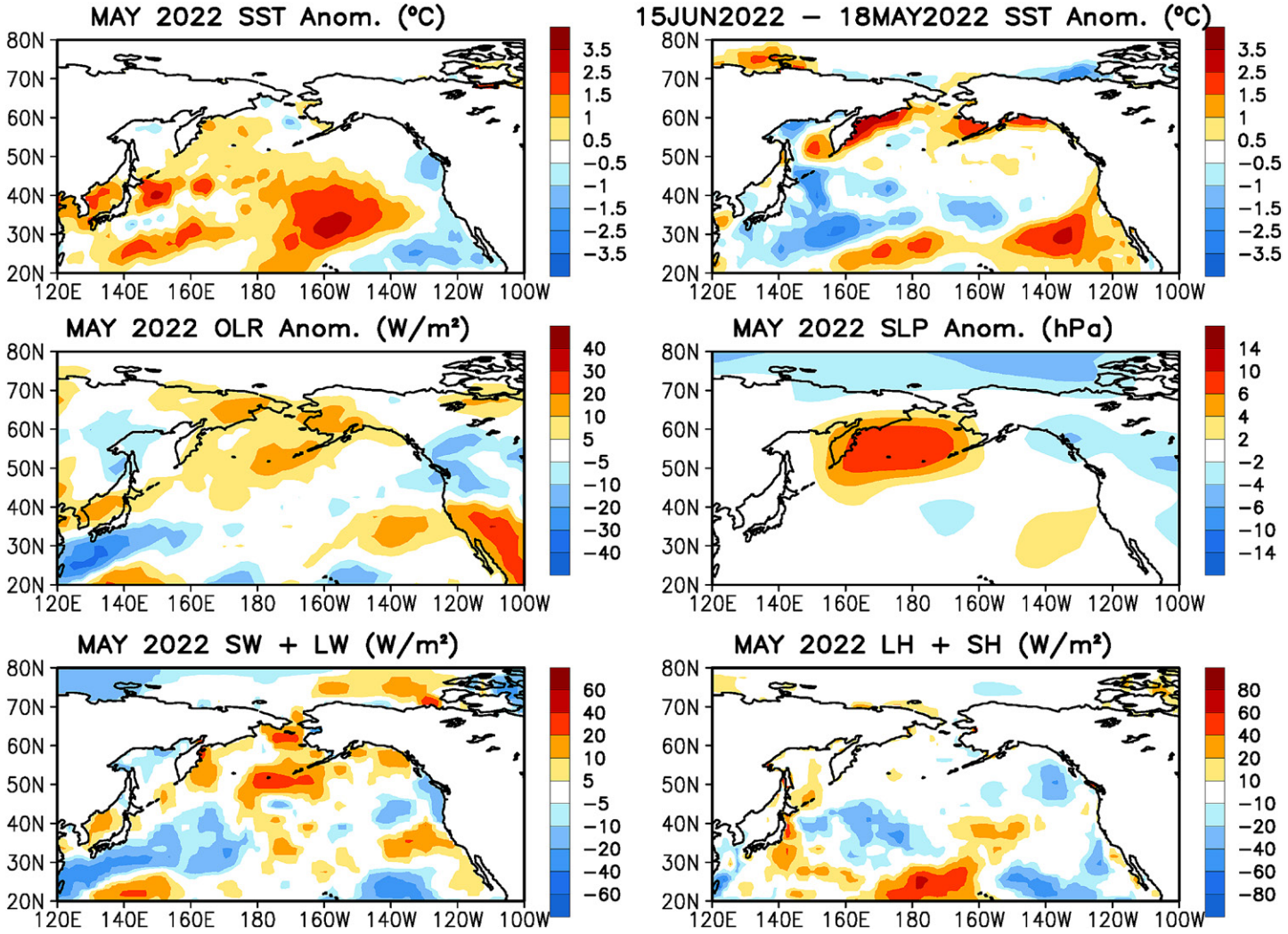

Fig. 5. OIv2.1 (top left) monthly SSTAs, (top right) weekly SSTA tendency, (middle left) OLR monthly anomalies, (middle right) SLP monthly anomalies, (bottom left) the sum of net surface short- and longwave radiation monthly anomalies, and (bottom right) the sum of latent and sensible heat flux monthly anomalies. Here, the weekly SSTA tendency is referred to the differences between weekly SSTA centered on 2 Mar 2022 and weekly SSTA centered on 2 Feb 2022. SST is derived from the OIv2.1, OLR from the *NOAA-18* Advanced Very High Resolution Radiometer (AVHRR) measurements, winds, surface radiation, and heat fluxes from the NCEP–NCAR reanalysis. Anomalies are departures from the 1991–2020 base period means.

Global ocean forecasts and global ocean observing system

Global ocean forecasts. Real-time monitoring efforts are complemented by their predictive counterparts. The real-time forecasts for modes of variability in each ocean basin are based on the forecasts of the NCEP CFSv2 (Saha et al. 2014; Xue et al. 2013; Zhu et al. 2015), which is initialized with the NCEP Climate Forecast System Reanalysis (Xue et al. 2012; Saha et al. 2010). In addition to the update of the CPC website dedicated to the CFSv2 seasonal and monthly forecasts associated with ENSO (www.cpc.ncep.noaa.gov/products/people/wwang/cfsv2fcst/), the forecasting component focuses on the indices including Niño-3.4, IOD, PDO, and TNA.

Figure 8 shows an example of the forecasts of the Niño-3.4 index. By comparing the evolution of the forecasts with different initial conditions during the last nine months, the tendencies of the model forecast are illustrated and are useful in developing the official ENSO, surface temperature, and precipitation forecasts at CPC. SSTA forecasts of CFSv2 in the North Pacific for different lead times are also routinely released to monitor the marine heatwave in the region. The forecasts of the TNA are useful input for developing the seasonal Atlantic hurricane outlook. It should be noted that compared with the prediction in the central and

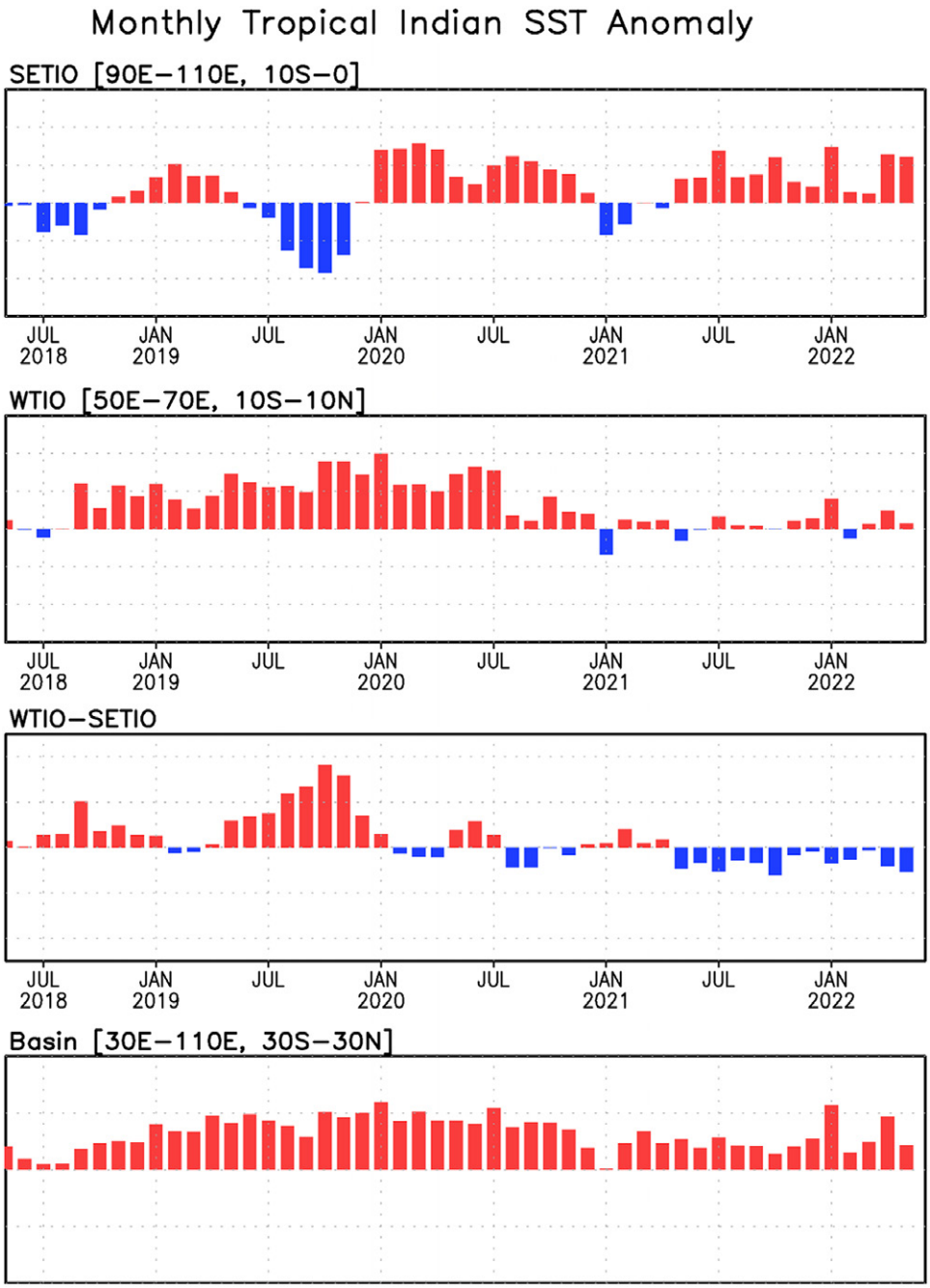

Fig. 6. Indian Ocean OIv2.1 SST indices, calculated as the area-averaged monthly SSTAs (°C) for the southeastern tropical Indian Ocean (SETIO; 90°–110°E, 10°S–0°) and western tropical Indian Ocean (WTIO; 50°–70°E, 10°S–10°N) regions, and dipole mode index, defined as differences between WTIO and SETIO. The basin mode index is the monthly SSTAs (°C) averaged over (30°–110°E, 30°S–30°N).

eastern tropical Pacific Ocean associated with ENSO, the prediction skill for the SSTA in the North Atlantic (Hu et al. 2013) and North Pacific (Hu et al. 2014) Oceans is much lower and a large contributor to the skill is due to the impact of ENSO.

In addition to SST predictions, CPC has devoted considerable efforts to forecasting sea ice (Wang et al. 2013). Through improving model physics and sea ice initial conditions, Arctic sea ice variation prediction is found to be more skillful. In the monthly ocean briefing, we discuss the CPC prediction of the Arctic sea ice extent in the next nine months and compare it with the observed climatological evolution in 1981–2010 (www.cpc.ncep.noaa.gov/products/people/wwang/seaice_seasonal/index.html).

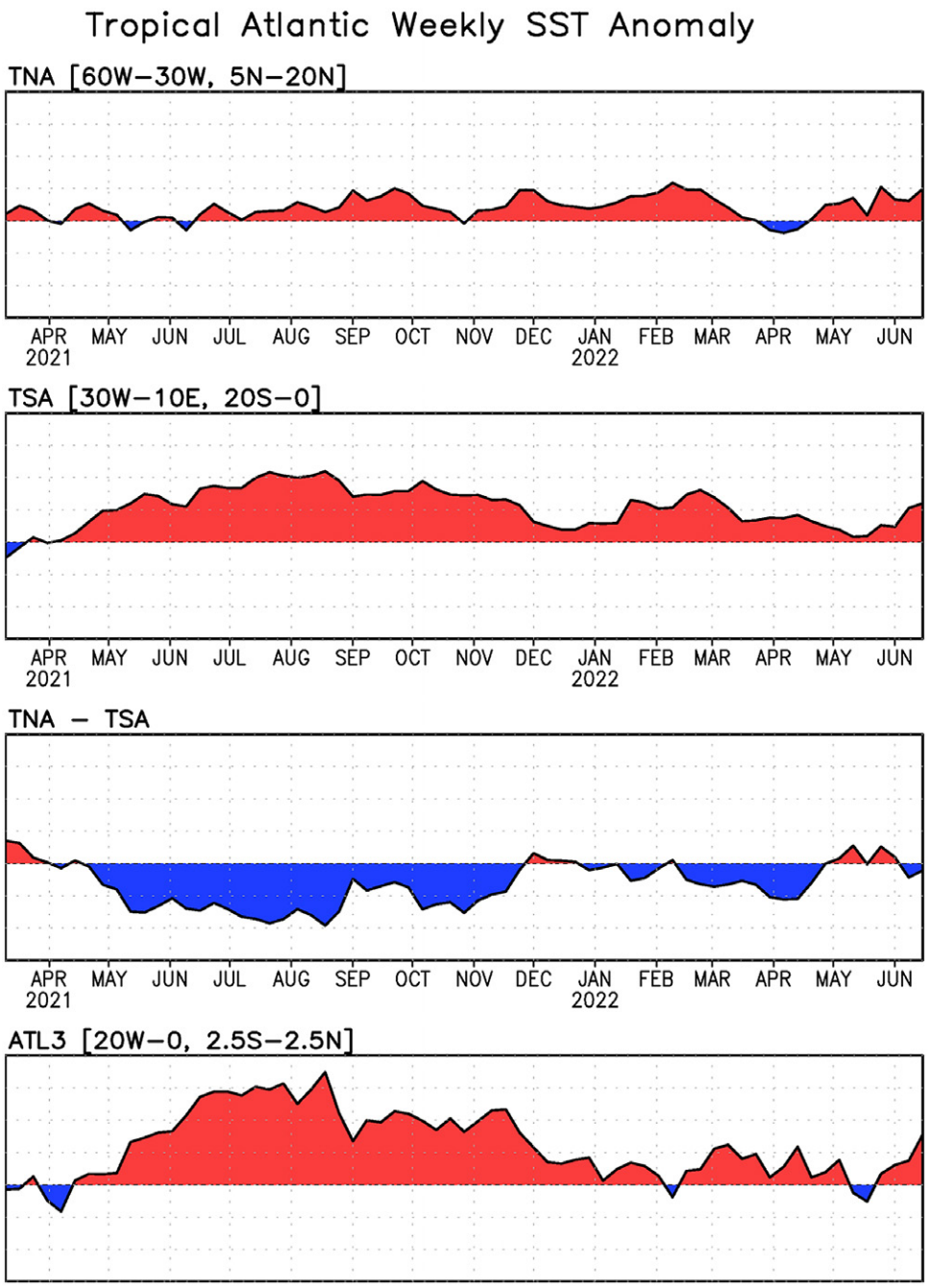

Fig. 7. Indices of tropical Atlantic weekly OIv2.1 SSTAs (°C): tropical North Atlantic (TNA; 60°–30°W, 5°–20°N), tropical South Atlantic (TSA; 30°W–10°E, 20°S–0°) and ATL3 regions, and meridional gradient index, defined as differences between TNA and TSA. The ATL3 index is SSTAs (°C) averaged over (20°W–0°, 2.5°S–2.5°N).

Global ocean observing system. In situ ocean observations from different platforms are the basis of real-time ocean monitoring and prediction (Capotondi et al. 2019). As a result of international cooperation, a robust in situ ocean observing system now exists (Moltmann et al. 2019). However, there is a need to continuously monitor the health of the ocean observing system for various reasons: incidents of vandalism could lead to regional observing gaps; what ocean observations are received at operations centers and included in ocean data assimilation. For example, 16 buoy failures in 2008 were attributed to vandal actions and vandalism approximately contributed a continuous 15%–20% impact on the TAO product quality between October 2007 and June 2008 (Teng et al. 2009). For these reasons, monitoring

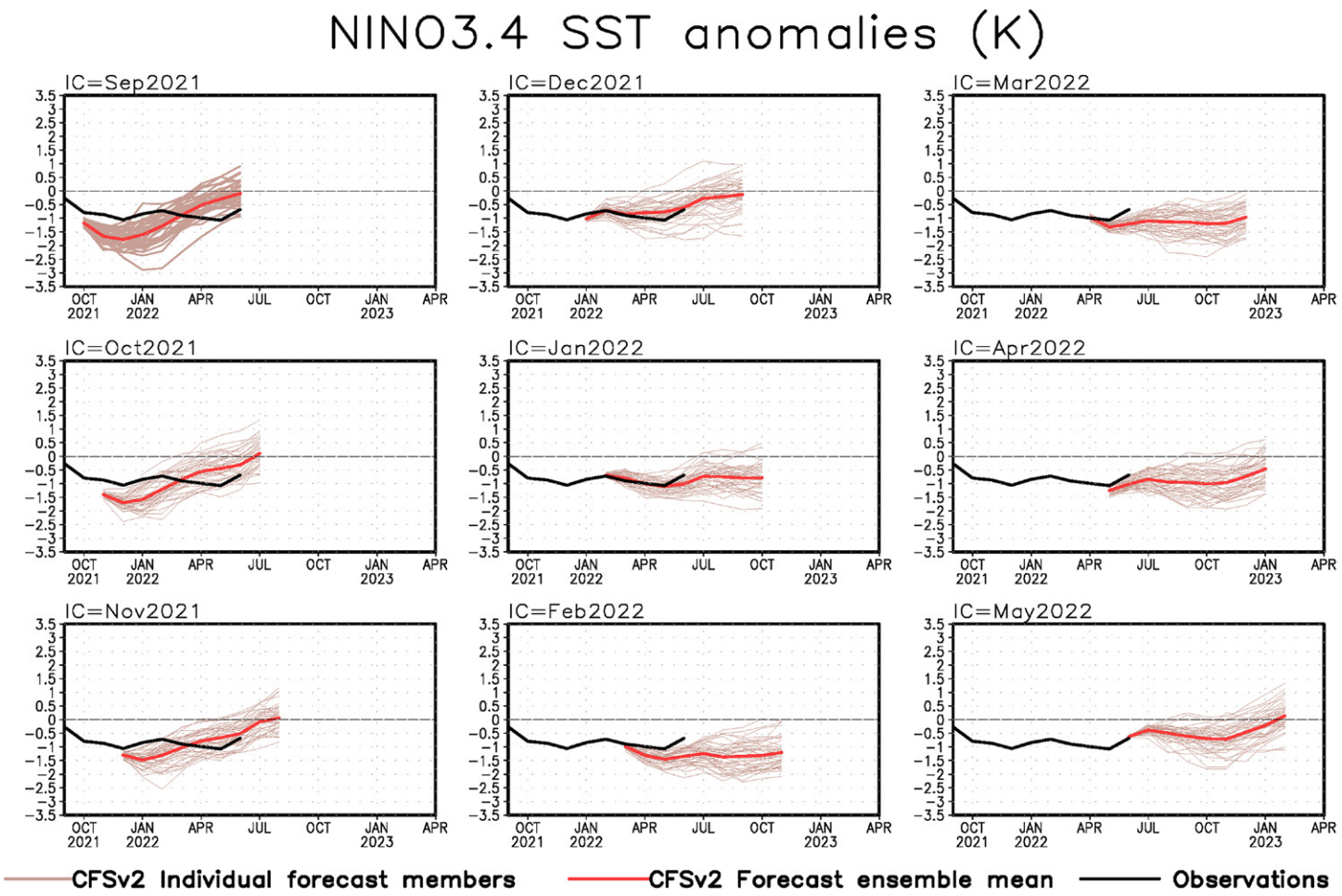

Fig. 8. CFSv2 predicted monthly Niño-3.4 SSTA (°C) from the latest 9 initial months. Displayed are 40 forecast members (brown) made four times per day initialized from the last 10 days of the initial month (labeled as IC=MonthYear) as well as the ensemble mean (red) and observations (OIv2.1; black).

of the availability of the ocean observing system from various platforms is desired and provided in CPC, and includes observational counts from TAO and Triangle Trans-Ocean Buoy Network (TRITON), expendable bathythermograph (XBT) transects, and the Argo profiling float network.

Ocean observing system monitoring products include spatial distribution of ocean temperature profiles, time series of daily ocean temperature profile numbers in the upper 300 m for the global oceans and the tropical Pacific Ocean (10°S–10°N, 120°E–80°W), as well as vertical distribution of the ocean temperature profile number in 3°S–3°N. As an example, Fig. 9 shows the time series of the number of daily ocean temperature profiles per month accumulated in the tropical Pacific from TAO/TRITON (red line), Argo (blue line), XBT (green line), and TAO/TRITON/Argo/XBT together (black line) since January 1979 (Xue et al. 2017). The time series is striking in the quick increase of the numbers of the Argo profiles during the last 20 years. Also evident in the time series for the number of TAO observations is a precipitous decline that occurred in 2013. As TAO moored array in the equatorial tropical Pacific is crucial for ENSO monitoring and prediction, this decline raised concerns in the community leading to the workshop on the Tropical Pacific Observing System 2020 (TPOS 2020) held in January 2014, at Scripps Institution of Oceanography, San Diego, United States. The purpose of the workshop was to evaluate the requirements and status of the ocean observing system in the tropical Pacific. Recommendations from the workshop resulted in the establishment TPOS 2020 Project (https://tropicalpacific.org) to build a robust and sustainable observing system to

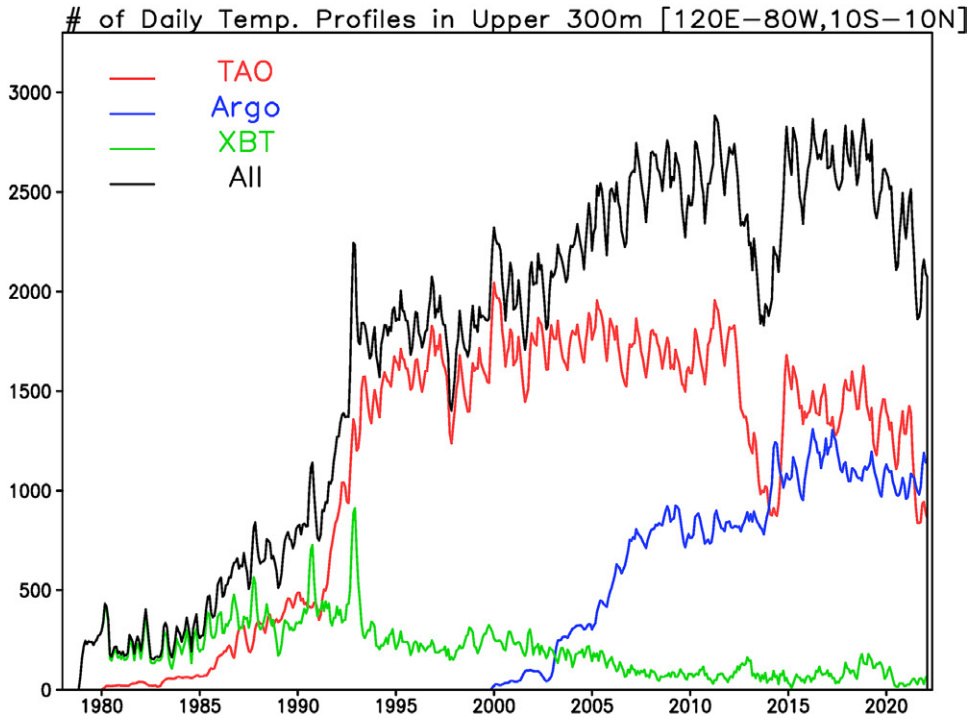

Fig. 9. Time series of the number of daily ocean temperature profiles per month accumulated in the tropical Pacific from the Tropical Atmosphere Ocean/Triangle Trans-Ocean Buoy Network (TAO/TRITON; red line), Argo (blue line), the expendable bathythermograph (XBT; green line), and TAO/TRITON/Argo/XBT together (black line) since January 1979.

meet existing and evolving observational requirements. Similar reviews for the Atlantic (Johns et al. 2021) and Indian (Beal et al. 2020) Oceans have also been completed. As the ocean observing system evolves in near future, a continuous need for monitoring ocean observations becomes even more critical.

Challenges of ocean monitoring and predictions

Analysis uncertainty. One of the challenges for ocean observing is quantifying the uncertainty. This uncertainty is reflected in disagreements among observation-based products. For example, Huang et al. (2013) noted that sometimes the differences of SSTA in the tropical Pacific between ERSSTv3b and OIv2 can be larger than 0.5°C. Such large uncertainties/biases in the SST data can lead to different categorizations of ENSO events (Huang et al. 2016; Hu et al. 2020b; Johnson et al. 2019). Similarly, large differences in surface wind stress are present among the different reanalyses (Xue et al. 2011; Wen et al. 2018). Kumar and Hu (2012) compared the SST–surface wind and heat flux feedbacks associated with ENSO in six reanalyses and noted appreciable differences in both the spatial pattern and intensity. Such uncertainties are either due to inadequate observations or biases in respective data assimilation systems (Xue et al. 2011; Huang et al. 2013, 2016).

Due to even fewer observations for the subsurface ocean, the differences are larger for the subsurface OTAs among different products (Xue et al. 2011, 2012). For example, there are noticeable differences of OTAs along the equatorial Pacific in the intensities of both the negative and positive anomalies as well as detailed structures of the anomalies among TAO, GODAS, and NCEP's CFSR (Saha et al. 2010; Xue et al. 2011; www.cpc.ncep.noaa.gov/products/people/zzhu/HU_cfsr_tao_godas_mnth_PACIFIC.gif). Hu and Kumar (2015) argued that the differences in ocean temperature between GODAS and CFSR are larger when the availability of the TAO mooring observations reduces. Reduction of the biases in the subsurface ocean temperature has been demonstrated to improve prediction skills of ENSO (Zhu et al. 2012) and regional

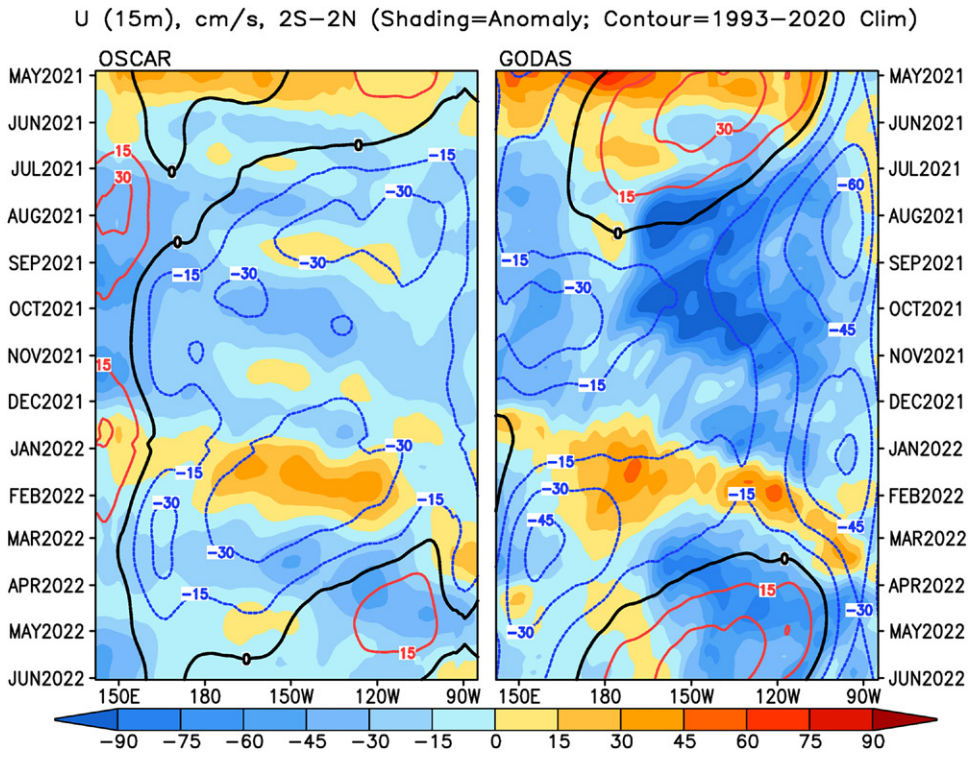

Fig. 10. Pentad zonal current anomalies (cm s^{-1}) averaged in 2°S–2°N from the (left) Ocean Surface Current Analysis Real-time (OSCAR) and (right) GODAS (shading) and the corresponding climatologies (contours; cm s^{-1}).

climate variability (Zhu et al. 2013). Also, a reduction in TAO observations might be potentially associated with the failure of some ENSO forecasts (McPhaden et al. 2015).

Such uncertainties also exist in other ocean monitoring products, such as SSH anomalies and near-surface zonal currents (Fig. 10). Ocean current plays an important role in ENSO evolution through zonal and meridional advection (Chen et al. 2016). In our monitoring efforts over the past 15 years, we noticed large differences in the near-surface zonal current anomalies (shading in Fig. 10) and in climatologies (contours in Fig. 10) between the satellite data (Dohan 2017) and GODAS analysis. Similarly, the differences of SSH anomalies among the satellite altimetry, GODAS, and CFSR are sometimes extremely large in the high latitudes of both the Northern and Southern Hemispheres, especially in the regions near the boundary between the open oceans and sea ice mass. Such differences may be largely due to the biases in the data assimilation systems and also partially caused by the errors in the satellite data.

From the differences among observational products, it is evident that uncertainties among them need to be quantified and conveyed to the users. One such effort developed in CPC is archiving multiple ocean reanalyses from various operational centers. Using multiple ocean analyses, we quantify the signal and uncertainty in the ocean temperature analysis (Xue et al. 2012). A similar effort for quantifying uncertainties in the SST analysis has also been established. As a part of the monthly ocean briefings, cases with large uncertainty among ocean products are often discussed.

Future directions of ocean monitoring and prediction efforts. CPC's ocean monitoring and prediction effort is continuously striving to enhance its scope and utility. For example, by including multiple analyzed SST data, the robustness of SSTA evolution can be illustrated. In the future, at the beginning of each ocean briefing, we plan to review major phenomena discussed in the previous month's briefing to give a sense of continuity of the developing physical events.

Another area of enhancement is to develop a suite of monitoring and prediction products to include additional ocean phenomena. One recent example attracting the community's attention is the long-lasting warm SST events in the extratropical Pacific Ocean. These events, often referred to as the "warm blob," occurred in 2014–16 and 2019 (Bond et al. 2015; Di Lorenzo and Mantua 2016; Hu et al. 2017; Amaya et al. 2020; Xu et al. 2020). Because of climate trends, the frequency of anomalous warm events is increasing. Given the societal impacts of long-lasting SST warming events, we intend to develop tools to monitor the evolution of marine heatwaves for global oceans with a focus on the North Pacific Ocean. With the expansion of ocean observations to more variables, in addition to sea surface salinity (Xie et al. 2014), future monitoring considerations may also include ocean color (Dutkiewicz et al. 2019), and ocean acidity (Guinotte and Fabry 2008).

Additional areas of enhancements in product delivery may also include providing diagnostics products for various facets of ocean variability and enhanced monitoring in the evolution of ocean observations. An example of diagnosis is our attempt to develop a suite of tools to understand the observed evolution of ENSO. Such an effort will include monitoring air–sea feedback contributing to ENSO evolution, heat budget analysis of ENSO SSTAs, the integrated influence of surface wind forcing in the equatorial Pacific, etc. The extratropical ENSO precursors, such as the Pacific meridional mode (PMM; Chiang and Vimont 2004) could also be included in the ocean briefing, as indications from climate projections suggest that PMM might increase under global warming (Liguori and Di Lorenzo 2018).

Monitoring the ocean observing system is important for continual assessment of the health of the observing system and, further, its possible influence on the quality of the ocean analysis as the observing system evolves. One of the TPOS 2020 Project recommendations is a reconfiguration of in situ ocean observing systems in the tropical Pacific, and as this effort develops, it will be important to quantify its influence on ocean analysis and prediction. Toward this, we are developing an effort to enhance monitoring of the ocean observing system, and together with the assessment of consistency among various ocean analysis products from operational centers, assessing its influence on the analysis uncertainty. Finally, toward improving and advancing CPC's ocean monitoring and prediction products, we are continuously seeking inputs from the external community for their ideas and suggestions.

All the ocean monitoring and forecast products are posted on the following web page and updated routinely ("www.cpc.ncep.noaa.gov/products/GODAS/ocean_briefing.shtml#Global"). The monthly briefing PPT files since 2007 are archived at "www.cpc.ncep.noaa.gov/products/GODAS/ocean_briefing_archive_ppt.shtml."

Acknowledgments. We thank the reviewers and our colleagues Drs. Hui Wang and Yanjuan Guo for their constructive comments and insightful suggestions. The Ocean Monitoring and Prediction Operations are also supported by many NCEP EMC and CPC colleagues, including David Behringer, Hyun-chul Lee, Bert Katz, Muthuvel Chelliah, Li Zhang, Wesley Ebisuzaki, and others, through maintaining GODAS, CFSR, NCEP R1 and R2 reanalyses, CFSv2 forecasts, and SST analyses. The scientific results and conclusions, as well as any view or opinions expressed herein, are those of the authors and do not necessarily reflect the views of NWS, NOAA, or the Department of Commerce. This project, to deliver real-time ocean monitoring products, is implemented by NOAA CPC in cooperation with NOAA's Global Ocean Monitoring and Observing Program (GOMO), United States.

Data availability statement. The ERSSTv5 and OIv2.1 SST data can be downloaded from "www.ncei.noaa.gov/products/extended-reconstructed-sst" (Huang et al. 2017) and "www.ncei.noaa.gov/products/optimum-interpolation-sst" (Huang et al. 2021), respectively. Atmospheric and GODAS reanalyses are

from "https://psl.noaa.gov/data/gridded/data.ncep.reanalysis.html" (Kalnay et al. 1996), "https://psl.noaa.gov/data/gridded/data.ncep.reanalysis2.html" (Kanamitsu et al. 2002), and "https://psl.noaa.gov/data/gridded/data.godas.html" (Behringer and Xue 2004), respectively. OLR data are available at "https://psl.noaa.gov/data/gridded/data.interp_OLR.html" (Liebmann and Smith 1996). The SSH and zonal current data for this research are included in Pujol et al. (2016) and Dohan (2017). The details of the data can be referred to in the appendix.

Appendix: Data

The monthly sea surface temperature (SST) data are from the Extended Reconstructed SST version 5 (ERSSTv5; Huang et al. 2017), and monthly and weekly SSTs are from daily Optimum Interpolation SST (OIv2.1; Huang et al. 2021). The SSH (Pujol et al. 2016) and zonal current data (Dohan 2017) are based on satellite retrieval of multimission altimeter data. The zonal component of wind at 850 hPa (U850) and vorticity potential at 200 hPa are from NCEP and the National Center for Atmospheric Research (NCAR) reanalysis (R1; Kalnay et al. 1996). Wind at 925 and 200 hPa, and heat flux are from NCEP and the Department of Energy (DOE) reanalysis (R2; Kanamitsu et al. 2002), and OLR data are from Liebmann and Smith (1996). All other variables are the outputs of the oceanic data assimilation from the GODAS (Behringer and Xue 2004). The monthly, weekly, and pentad anomalies are currently referred to the corresponding climatologies in 1991–2020, which are updated every 10 years.

The tropical cyclone heat potential (TCHP) is defined as the total OHC above the 26°C isotherm, which is a potential energy source for tropical cyclone geneses and growth. The ocean mixed layer depth is defined as the depth where the oceanic temperature deviation from the surface temperature is less than 0.8°C based on the oceanic temperature of GODAS (Huang et al. 2010), which is used to monitor the thermocline fluctuation along the equator associated with Kelvin wave activity, a trigger for ENSO initiation.

The forecasts are from the CFSv2 (Saha et al. 2014), which includes 40 ensemble members with a 9-month range made four times per day with initial conditions from the CFSR (Saha et al. 2010) of the last 10 days of the initial month.

References

Amaya, D. J., A. J. Miller, S.-P. Xie, and Y. Kosaka, 2020: Physical drivers of the summer 2019 North Pacific marine heatwave. *Nat. Commun.*, **11**, 1903, https://doi.org/10.1038/s41467-020-15820-w.

Ashok, K., S. K. Behera, S. A. Rao, H. Weng, and T. Yamagata, 2007: El Niño Modoki and its possible teleconnection. *J. Geophys. Res.*, **112**, C11007, https://doi.org/10.1029/2006JC003798.

Barnston, A. G., and R. E. Livezey, 1987: Classification, seasonality and persistence of low-frequency atmospheric circulation patterns. *Mon. Wea. Rev.*, **115**, 1083–1126, https://doi.org/10.1175/1520-0493(1987)115<1083:CSAPOL>2.0.CO;2.

——, M. Chelliah, and S. B. Goldenberg, 1997: Documentation of a highly ENSO-related SST region in the equatorial Pacific. *Atmos.–Ocean*, **35**, 367–383, https://doi.org/10.1080/07055900.1997.9649597.

Beal, L. M., and Coauthors, 2020: A road map to IndOOS-2: Better observations of the rapidly warming Indian Ocean. *Bull. Amer. Meteor. Soc.*, **101**, E1891–E1913, https://doi.org/10.1175/BAMS-D-19-0209.1.

Behringer, D. W., and Y. Xue, 2004: Evaluation of the Global Ocean Data Assimilation System at NCEP: The Pacific Ocean. *Eighth Symp. on Integrated Observing and Assimilation Systems for Atmosphere, Oceans, and Land Surface*, Seattle, WA, Amer. Meteor. Soc., 2.3, http://ams.confex.com/ams/84Annual/techprogram/paper_70720.htm.

Bojinski, S., M. Verstraete, T. Peterson, C. Richter, A. Simmons, and M. Zemp, 2014: The concept of essential climate variables in support of climate research, applications, and policy. *Bull. Amer. Meteor. Soc.*, **95**, 1431–1443, https://doi.org/10.1175/BAMS-D-13-00047.1.

Bond, N. A., M. F. Cronin, H. Freeland, and N. Mantua, 2015: Causes and impacts of the 2014 warm anomaly in the NE Pacific. *Geophys. Res. Lett.*, **42**, 3414–3420, https://doi.org/10.1002/2015GL063306.

Capotondi, A., and Coauthors, 2019: Observational needs supporting marine ecosystems modeling and forecasting: From the global ocean to regional and coastal systems. *Front. Mar. Sci.*, **6**, 623, https://doi.org/10.3389/fmars.2019.00623.

Chambers, D. P., B. D. Tapley, and R. H. Stewart, 1999: Anomalous warming in the Indian Ocean coincident with El Niño. *J. Geophys. Res.*, **104**, 3035–3047, https://doi.org/10.1029/1998JC900085.

Chen, H.-C., Z.-Z. Hu, B. Huang, and C.-H. Sui, 2016: The role of reversed equatorial zonal transport in terminating an ENSO event. *J. Climate*, **29**, 5859–5877, https://doi.org/10.1175/JCLI-D-16-0047.1.

Cherchi, A., S. Gualdi, S. Behera, J. J. Luo, S. Masson, T. Yamagata, and A. Navarra, 2007: The influence of tropical Indian Ocean SST on the Indian summer monsoon. *J. Climate*, **20**, 3083–3105, https://doi.org/10.1175/JCLI4161.1.

Chiang, J. C. H., and D. J. Vimont, 2004: Analogous Pacific and Atlantic meridional modes of tropical atmosphere–ocean variability. *J. Climate*, **17**, 4143–4158, https://doi.org/10.1175/JCLI4953.1.

Di Lorenzo, E., and N. Mantua, 2016: Multi-year persistence of the 2014/15 North Pacific marine heatwave. *Nat. Climate Change*, **6**, 1042–1047, https://doi.org/10.1038/nclimate3082.

Dohan, K., 2017: Ocean surface currents from satellite data. *J. Geophys. Res. Oceans*, **122**, 2647–2651, https://doi.org/10.1002/2017JC012961.

Dutkiewicz, S., A. E. Hickman, O. Jahn, S. Henson, C. Beaulieu, and E. Monier, 2019: Ocean colour signature of climate change. *Nat. Commun.*, **10**, 578, https://doi.org/10.1038/s41467-019-08457-x.

Enfield, D. B., A. M. Mestas, D. A. Mayer, and L. Cid-Serrano, 1999: How ubiquitous is the dipole relationship in tropical Atlantic sea surface temperatures? *J. Geophys. Res.*, **104**, 7841–7848, https://doi.org/10.1029/1998JC900109.

Fujii, Y., and Coauthors, 2019: Observing system evaluation based on ocean data assimilation and prediction systems: On-going challenges and a future vision for designing and supporting ocean observational networks. *Front. Mar. Sci.*, **6**, 417, https://doi.org/10.3389/fmars.2019.00417.

Gray, W. M., 1984: Atlantic seasonal hurricane frequency: Part I: El Niño and 30-mb quasi-biennial oscillation influences. *Mon. Wea. Rev.*, **112**, 1649–1668, https://doi.org/10.1175/1520-0493(1984)112<1649:ASHFPI>2.0.CO;2.

Guinotte, J. M., and V. J. Fabry, 2008: Ocean acidification and its potential effects on marine ecosystems. *Ann. N. Y. Acad. Sci.*, **1134**, 320–342, https://doi.org/10.1196/annals.1439.013.

Han, R., and Coauthors, 2016: An assessment of multi-model simulations for the variability of western North Pacific tropical cyclones and its association with ENSO. *J. Climate*, **29**, 6401–6423, https://doi.org/10.1175/JCLI-D-15-0720.1.

Hu, Z.-Z., and A. Kumar, 2015: Influence of availability of TAO data on NCEP ocean data assimilation systems along the equatorial Pacific. *J. Geophys. Res. Oceans*, **120**, 5534–5544, https://doi.org/10.1002/2015JC010913.

——, ——, B. Huang, W. Wang, J. Zhu, and C. Wen, 2013: Prediction skill of monthly SST in the North Atlantic Ocean in NCEP Climate Forecast System version 2. *Climate Dyn.*, **40**, 2745–2759, https://doi.org/10.1007/s00382-012-1431-z.

——, ——, ——, J. Zhu, and Y. Guan, 2014: Prediction skill of North Pacific variability in NCEP Climate Forecast System version 2: Impact of ENSO and beyond. *J. Climate*, **27**, 4263–4272, https://doi.org/10.1175/JCLI-D-13-00633.1.

——, ——, and ——, 2016: Spatial distribution and the interdecadal change of leading modes of heat budget of the mixed-layer in the tropical Pacific and the association with ENSO. *Climate Dyn.*, **46**, 1753–1768, https://doi.org/10.1007/s00382-015-2672-4.

——, ——, B. Jha, J. Zhu, and B. Huang, 2017: Persistence and predictions of the remarkable warm anomaly in the northeastern Pacific Ocean during 2014–2016. *J. Climate*, **30**, 689–702, https://doi.org/10.1175/JCLI-D-16-0348.1.

——, ——, ——, and B. Huang, 2020a: How much of monthly mean precipitation variability over global land is associated with SST anomalies? *Climate Dyn.*, **54**, 701–712, https://doi.org/10.1007/s00382-019-05023-5.

——, M. J. McPhaden, A. Kumar, J.-Y. Yu, and N. C. Johnson: 2020b: Uncoupled El Niño warming. *Geophys. Res. Lett.*, **47**, e2020GL08762, https://doi.org/10.1029/2020GL087621.

Huang, B., Y. Xue, D. Zhang, A. Kumar, and M. J. McPhaden, 2010: The NCEP GODAS ocean analysis of the tropical Pacific mixed layer heat budget on seasonal to interannual time scales. *J. Climate*, **23**, 4901–4925, https://doi.org/10.1175/2010JCLI3373.1.

——, ——, H. Wang, W. Wang, and A. Kumar, 2012: Mixed layer heat budget of the El Niño in NCEP Climate Forecast System. *Climate Dyn.*, **39**, 365–381, https://doi.org/10.1007/s00382-011-1111-4.

——, M. L'Heureux, J. Lawrimore, C. Liu, H.-M. Zhang, V. Banzon, Z.-Z. Hu, and A. Kumar, 2013: Why did large differences arise in the sea surface temperature datasets across the tropical Pacific during 2012? *J. Atmos. Oceanic Technol.*, **30**, 2944–2953, https://doi.org/10.1175/JTECH-D-13-00034.1.

——, ——, Z.-Z. Hu, and H.-M. Zhang, 2016: Ranking the strongest ENSO events while incorporating SST uncertainty. *Geophys. Res. Lett.*, **43**, 9165–9172, https://doi.org/10.1002/2016GL070888.

——, and Coauthors, 2017: Extended Reconstructed Sea Surface Temperature version 5 (ERSSTv5): Upgrades, validations, and intercomparisons. *J. Climate*, **30**, 8179–8205, https://doi.org/10.1175/JCLI-D-16-0836.1.

——, C. Liu, V. Banzon, E. Freeman, G. Graham, B. Hankins, T. Smith, and H.-M. Zhang, 2021: Improvements of the Daily Optimum Interpolation Sea Surface Temperature (DOISST) version 2.1. *J. Climate*, **34**, 2923–2939, https://doi.org/10.1175/JCLI-D-20-0166.1.

Jin, F.-F., 1997: An equatorial ocean recharge paradigm for ENSO. Part I: Conceptual model. *J. Atmos. Sci.*, **54**, 811–829, https://doi.org/10.1175/1520-0469(1997)054<0811:AEORPF>2.0.CO;2.

Johns, W., and Coauthors, 2021: Tropical Atlantic Observing System (TAOS) Review Report. CLIVAR Rep., 218 pp.

Johnson, N. C., M. L. L'Heureux, C.-H. Chang, and Z.-Z. Hu, 2019: On the delayed coupling between ocean and atmosphere in recent weak El Niño

episodes. *Geophys. Res. Lett.*, **46**, 11 416–11 425, https://doi.org/10.1029/2019GL084021.

Kalnay, E., and Coauthors, 1996: The NCEP/NCAR 40-Year Reanalysis Project. *Bull. Amer. Meteor. Soc.*, **77**, 437–471, https://doi.org/10.1175/1520-0477(1996)077<0437:TNYRP>2.0.CO;2.

Kanamitsu, M., W. Ebisuzaki, J. Woollen, S.-K. Yang, J. J. Hnilo, M. Fiorino, and G. L. Potter, 2002: NCEP-DOE AMIP-II Reanalysis (R-2). *Bull. Amer. Meteor.*, **83**, 1631–1644, https://doi.org/10.1175/BAMS-83-11-1631.

Kumar, A., and Z.-Z. Hu, 2012: Uncertainty in the ocean–atmosphere feedbacks associated with ENSO in the reanalysis products. *Climate Dyn.*, **39**, 575–588, https://doi.org/10.1007/s00382-011-1104-3.

——, and ——, 2014: Interannual and interdecadal variability of ocean temperature along the equatorial Pacific in conjunction with ENSO. *Climate Dyn.*, **42**, 1243–1258, https://doi.org/10.1007/s00382-013-1721-0.

——, and C. Wen, 2016: An oceanic heat content–based definition for the Pacific decadal oscillation. *Mon. Wea. Rev.*, **144**, 3977–3984, https://doi.org/10.1175/MWR-D-16-0080.1.

Li, X., Z.-Z. Hu, B. Huang, and C. Stan, 2022: Bulk connectivity of global SST and land precipitation variations. *Climate Dyn.*, **58**, 195–209, https://doi.org/10.1007/s00382-021-05901-x.

Liebmann, B., and C. A. Smith, 1996: Description of a complete (interpolated) outgoing longwave radiation dataset. *Bull. Amer. Meteor. Soc.*, **77**, 1275–1277, https://doi.org/10.1175/1520-0477-77.6.1274.

Liguori, G., and E. Di Lorenzo, 2018: Meridional modes and increasing Pacific decadal variability under anthropogenic forcing. *Geophys. Res. Lett.*, **45**, 983–991, https://doi.org/10.1002/2017GL076548.

Mantua, N. J., S. R. Hare, Y. Zhang, J. M. Wallace, and R. C. Francis, 1997: A Pacific interdecadal climate oscillation with impacts on salmon production. *Bull. Amer. Meteor. Soc.*, **78**, 1069–1079, https://doi.org/10.1175/1520-0477(1997)078<1069:APICOW>2.0.CO;2.

McPhaden, M. J., and Coauthors, 1998: The Tropical Ocean-Global Atmosphere (TOGA) observing system: A decade of progress. *J. Geophys. Res.*, **103**, 14 169–14 240, https://doi.org/10.1029/97JC02906.

——, A. Timmermann, M. J. Widlansky, M. A. Balmaseda, and T. N. Stockdale, 2015: The curious case of the El Niño that never happened: A perspective from 40 years of progress in climate research and forecasting. *Bull. Amer. Meteor. Soc.*, **96**, 1647–1665, https://doi.org/10.1175/BAMS-D-14-00089.1.

——, A. Santoso, and W. Cai, 2021: *El Niño Southern Oscillation in a Changing Climate. Geophys. Monogr.*, Vol. 253, Amer. Geophys. Union, 506 pp.

Meinen, C. S., and M. J. McPhaden, 2000: Observations of warm water volume changes in the equatorial Pacific and their relationship to El Niño and La Niña. *J. Climate*, **13**, 3551–3559, https://doi.org/10.1175/1520-0442(2000)013<3551:OOWWVC>2.0.CO;2.

Moltmann, T., and Coauthors, 2019: A global ocean observing system (GOOS), delivered through enhanced collaboration across regions, communities, and new technologies. *Front. Mar. Sci.*, **6**, 291, https://doi.org/10.3389/fmars.2019.00291.

National Research Council, 2010: *Assessment of Intraseasonal to Interannual Climate Prediction and Predictability*. National Academies Press, 192 pp.

Pujol, M.-I., Y. Faugère, G. Taburet, S. Dupuy, C. Pelloquin, M. Ablain, and N. Picot, 2016: DUACS DT2014: The new multi-mission altimeter data set reprocessed over 20 years. *Ocean Sci.*, **12**, 1067–1090, https://doi.org/10.5194/os-12-1067-2016.

Rasmusson, E. M., and T. H. Carpenter, 1983: The relationship between eastern equatorial Pacific sea surface temperature and rainfall over India and Sri Lanka. *Mon. Wea. Rev.*, **111**, 517–528, https://doi.org/10.1175/1520-0493(1983)111<0517:TRBEEP>2.0.CO;2.

Ren, H.-L., and F.-F. Jin, 2011: Niño indices for two types of ENSO. *Geophys. Res. Lett.*, **38**, L04704, https://doi.org/10.1029/2010GL046031.

Roemmich, D., and Coauthors, 2019: On the future of Argo: A global, full-depth, multi-disciplinary array. *Front. Mar. Sci.*, **6**, 439, https://doi.org/10.3389/fmars.2019.00439.

Ropelewski, C., and M. Halpert, 1987: Global and regional scale precipitation patterns associated with the El Niño/Southern Oscillation. *Mon. Wea. Rev.*, **115**, 1606–1626, https://doi.org/10.1175/1520-0493(1987)115<1606:GARSPP>2.0.CO;2.

Saha, S., and Coauthors, 2010: The NCEP Climate Forecast System Reanalysis. *Bull. Amer. Meteor. Soc.*, **91**, 1015–1058, https://doi.org/10.1175/2010BAMS3001.1.

——, and Coauthors, 2014: The NCEP Climate Forecast System version 2. *J. Climate*, **27**, 2185–2208, https://doi.org/10.1175/JCLI-D-12-00823.1.

Saji, N. H., B. N. Goswami, P. N. Vinayachandran, and T. Yamagata, 1999: A dipole mode in the tropical Indian Ocean. *Nature*, **401**, 360–363, https://doi.org/10.1038/43854.

Seo, K.-H., and Y. Xue, 2005: MJO-related oceanic Kelvin waves and the ENSO cycle: A study with the NCEP Global Ocean Data Assimilation System. *Geophys. Res. Lett.*, **32**, L07712, https://doi.org/10.1029/2005GL022511.

Teng, C., S. Cucullu, S. McArthur, C. Kohler, B. Burnett, and L. Bernard, 2009: Buoy vandalism experienced by NOAA National Data Buoy Center. *Oceans 2009*, Biloxi, MS, IEEE, https://doi.org/10.23919/OCEANS.2009.5422389.

van Oldenborgh, G. J., H. Hendon, T. Stockdale, M. L'Heureux, E. C. de Perez, R. Singh, and M. van Aalst, 2021: Defining El Niño indices in a warming climate. *Environ. Res. Lett.*, **16**, 044003, https://doi.org/10.1088/1748-9326/abe9ed.

Wang, H., and Coauthors, 2014: How well do global climate models simulate the variability of Atlantic tropical cyclones associated with ENSO? *J. Climate*, **27**, 5673–5692, https://doi.org/10.1175/JCLI-D-13-00625.1.

Wang, W., M. Chen, and A. Kumar, 2013: Seasonal prediction of Arctic sea ice extent from a coupled dynamical forecast system. *Mon. Wea. Rev.*, **141**, 1375–1394, https://doi.org/10.1175/MWR-D-12-00057.1.

Ware, D. M., and G. A. McFarlane, 1989: Fisheries production domains in the northeast Pacific Ocean. *Can. J. Fish. Aquat. Sci.*, **108**, 359–379.

Wen, C., A. Kumar, and Y. Xue, 2018: Uncertainties in reanalysis surface wind stress and their relationship with observing systems. *Climate Dyn.*, **52**, 3061–3078, https://doi.org/10.1007/s00382-018-4310-4.

Wu, R., Z.-Z. Hu, and B. P. Kirtman, 2003: Evolution of ENSO-related rainfall anomalies in East Asia. *J. Climate*, **16**, 3742–3758, https://doi.org/10.1175/1520-0442(2003)016<3742:EOERAI>2.0.CO;2.

Xie, P., and Coauthors, 2014: An in situ-satellite blended analysis of global sea surface salinity. *J. Geophys. Res. Oceans*, **119**, 6140–6160, https://doi.org/10.1002/2014JC010046.

Xu, T., M. Newman, A. Capotondi, and E. Di Lorenzo, 2020: The continuum of northeast Pacific marine heatwaves and their relationship to the tropical Pacific. *Geophys. Res. Lett.*, **48**, e2020GL090661, https://doi.org/10.1029/2020GL090661.

Xue, Y., B. Huang, Z.-Z. Hu, A. Kumar, C. Wen, D. Behringer, and S. Nadiga, 2011: An assessment of oceanic variability in the NCEP Climate Forecast System Reanalysis. *Climate Dyn.*, **37**, 2511–2539, https://doi.org/10.1007/s00382-010-0954-4.

——, and Coauthors, 2012: A comparative analysis of upper-ocean heat content variability from an ensemble of operational ocean reanalyses. *J. Climate*, **25**, 6905–6929, https://doi.org/10.1175/JCLI-D-11-00542.1.

——, M. Chen, A. Kumar, Z.-Z. Hu, and W. Wang, 2013: Prediction skill and bias of tropical Pacific sea surface temperatures in the NCEP Climate Forecast System version 2. *J. Climate*, **26**, 5358–5378, https://doi.org/10.1175/JCLI-D-12-00600.1.

——, C. Wen, X. Yang, D. Behringer, A. Kumar, G. Vecchi, A. Rosati, and R. Gudgel, 2017: Evaluation of tropical Pacific observing systems using NCEP and GFDL ocean data assimilation systems. *Climate Dyn.*, **49**, 843–868, https://doi.org/10.1007/s00382-015-2743-6.

Zebiak, S. E., 1993: Air–sea interaction in the equatorial Atlantic region. *J. Climate*, **6**, 1567–1586, https://doi.org/10.1175/1520-0442(1993)006<1567:AIITEA>2.0.CO;2.

Zhu, J., B. Huang, L. Marx, J. L. Kinter III, M. A. Balmaseda, R.-H. Zhang, Z.-Z. Hu, 2012: Ensemble ENSO hindcasts initialized from multiple ocean analyses. *Geophys. Res. Lett.*, **39**, L09602, https://doi.org/10.1029/2012GL051503.

——, ——, Z.-Z. Hu, J. L. Kinter III, and L. Marx, 2013: Predicting U.S. summer precipitation using NCEP Climate Forecast System version 2 initialized by multiple ocean analyses. *Climate Dyn.*, **41**, 1941–1954, https://doi.org/10.1007/s00382-013-1785-x.

——, ——, A. Kumar, and J. L. Kinter III, 2015: Seasonality in prediction skill and predictable pattern of tropical Indian Ocean SST. *J. Climate*, **28**, 7962–7984, https://doi.org/10.1175/JCLI-D-15-0067.1.